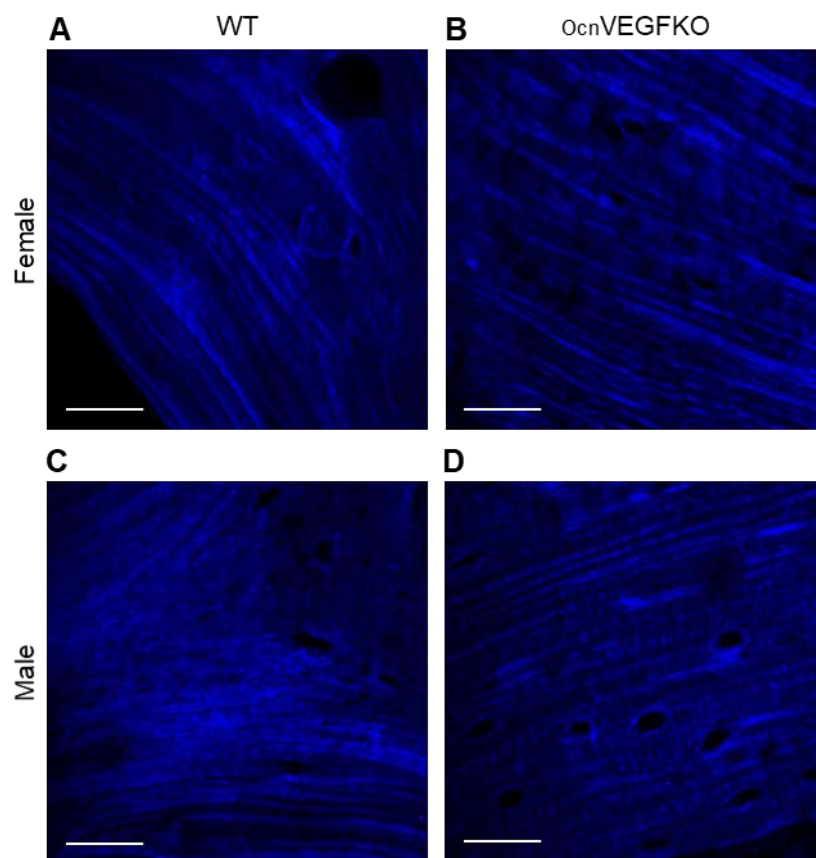
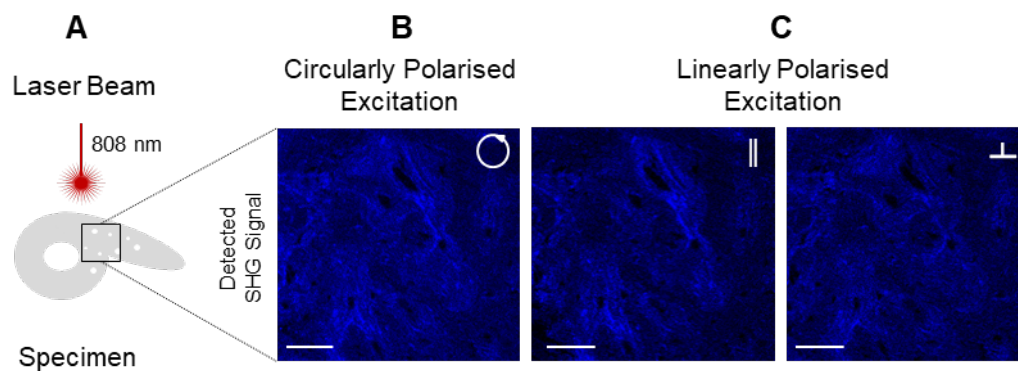


### Supplementary Information



**Fig. S1.** High magnification p-SHG images of PMMA embedded sections reveal collagen fibres in female WT (A), female OcnVEGFKO (B), male WT (C) and male OcnVEGFKO (D) sections. Scale bars represent 50  $\mu$ m.



**Fig. S2.** Visualisation of bone matrix collagen fibres is polarisation dependent. SHG images of PMMA embedded sections were acquired by tuning the wavelength of the fundamental excitation laser to 808 nm (A). Circular polarisation of the fundamental beam, achieved by modulation of  $\lambda/4$  and  $\lambda/2$  waveplates, enabled uniform excitation of collagen fibrils (B) orientated in all directions across the specimen. Linear polarisation enables excitation of collagen fibrils that are orientated parallel (C; ||, left) or orthogonal (C;  $\perp$ , right) to polarisation of the fundamental laser, showing maximum intensity with alignment at  $0^\circ$  (||) and minimum at  $90^\circ$  ( $\perp$ ). Scale bars represent  $50\ \mu\text{m}$ .

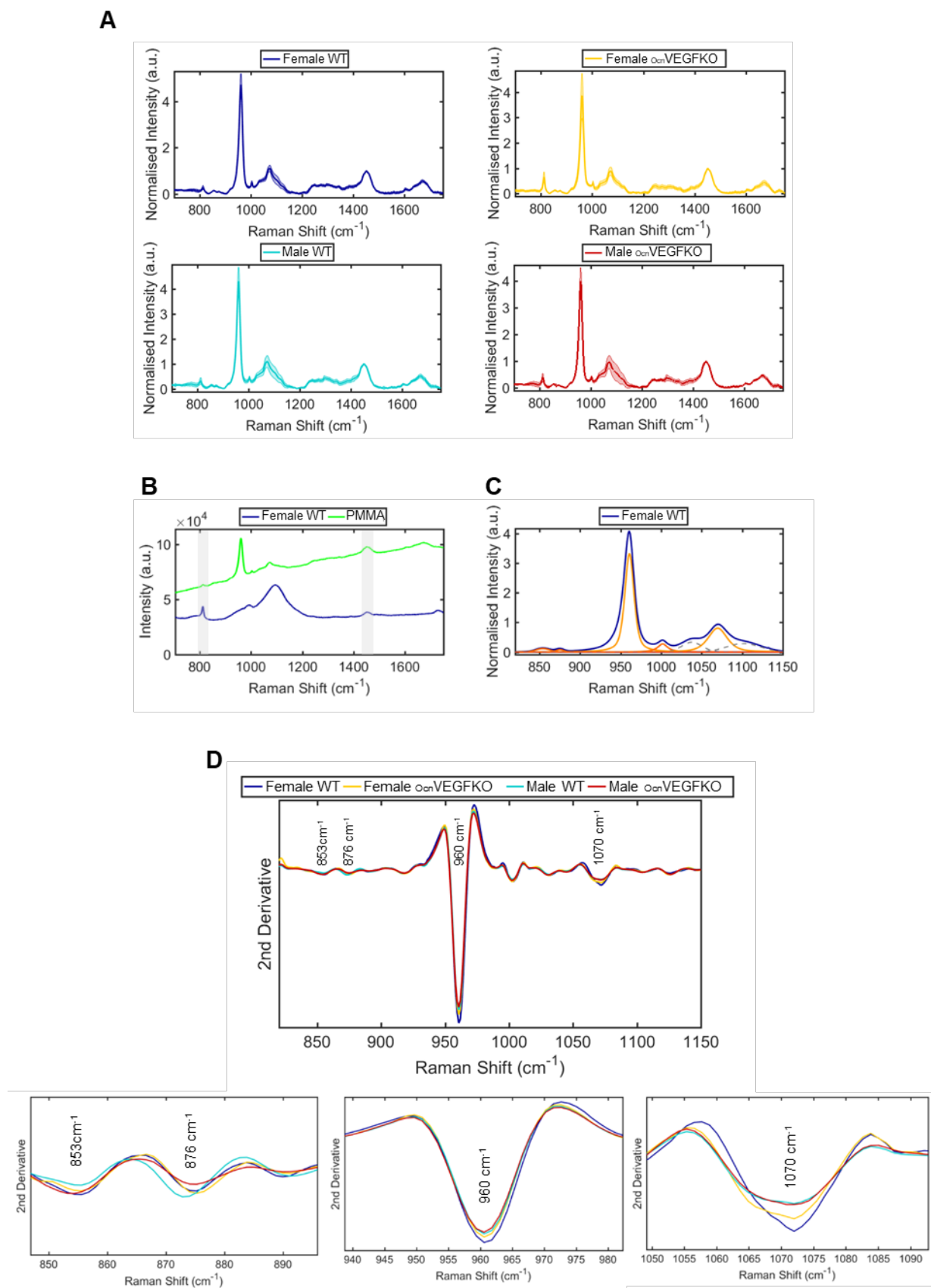


**Fig. S3.** Raman spectra collected within the fingerprint region from 700  $\text{cm}^{-1}$  to 1750  $\text{cm}^{-1}$  from the posterior region of three littermate matched female WT, female *OcnVEGFKO*, male WT and male *OcnVEGFKO* TFJ sections are presented as class means of  $n=75$  single spectra with SD displayed (A).

PMMA contributions in bone Raman spectra are highlighted in raw, unprocessed spectra ahead of deconvolution analysis. Peaks of interest associated with the ECM (proline, 853  $\text{cm}^{-1}$  and hydroxyproline, 876  $\text{cm}^{-1}$  in type I collagen) and mineral (HA, 960  $\text{cm}^{-1}$  and B-type carbonate, 1070  $\text{cm}^{-1}$ ), displayed as orange lines (C) are identifiable in bone Raman spectra following the calculation of second derivative spectra (D). Zoomed spectral peaks of interest identified in the second derivative spectra shown underneath (D) were analysed further by spectral deconvolution.